ISSUES AND R&D CRITICAL TO THE LCLS*

P. Emma§
Stanford Linear Accelerator Center, Stanford, CA 94309, USA

Abstract

The Linac Coherent Light Source (LCLS) [1] is a high brightness *x*-ray free-electron laser project based on the SLAC linac. A new photocathode rf gun serves as injector for the last kilometer of the linac, which is fitted with two-stages of bunch compression. Acceleration to 15-GeV produces intense 1.5-Å coherent radiation by self-amplified spontaneous emission in a long undulator. A multi-laboratory project collaboration is addressing the most challenging issues [2], including: 1) feasibility of a stable injector with normalized emittance of 1 μm at 1 nC; 2) emittance control in the linac including effects of coherent synchrotron radiation in the bunch compressors; 3) stability of the final electron beam in the presence of charge, timing, and energy variations; 4) design, construction and alignment of a long planar undulator with 3-cm period and discrete periodic focusing lattice; 5) understanding and control of wakefields due to wall surface roughness in the undulator vacuum chamber; 6) radiation-matter interactions in the strong field regime with mirror and crystal optics for filtering and deflecting. These issues, and a project update, are presented.

1 INTRODUCTION

The LCLS is an *x*-ray free-electron laser (FEL) based on the principal of self-amplified spontaneous emission (SASE) and supported by the SLAC linac. The R&D effort is a multi-laboratory collaboration including ANL, BNL, LANL, LLNL, SLAC, and UCLA.

Table 1. LCLS parameters at 1.5 Å radiation wavelength.

bunch charge	Q	1	nC
norm. 'slice' emittance	$\gamma\varepsilon_x/\gamma\varepsilon_y$	1.2	μm
final electron energy	E	14.35	GeV
final rms energy spread	σ_δ	0.02	%
final rms bunch length	σ_z	22	μm
peak current	I_{pk}	3.4	kA
peak brightness	B_{pk}	1.2×10^{33}	*
saturation length	L_{sat}	87	m
saturation power	P_{sat}	9-16	GW

* photons/s/mm^2/mrad^2/0.1%-BW

Table 1 lists the basic LCLS parameters at the shortest wavelength. Longer wavelength operation is also envisioned; from 1.5 Å at 14.35 GeV to 15 Å at 4.54 GeV.

* Work supported by DOE contract DE-AC03-76SF00515.
§ Emma@SLAC.Stanford.edu

2 INJECTOR

2.1 LCLS Injector Design

The LCLS injector is a 1.6-cell S-band RF photo-cathode gun [3] followed by a booster linac composed of two 3-meter S-band accelerating structures and a 45° bend system leading into the SLAC linac (Figure 1).

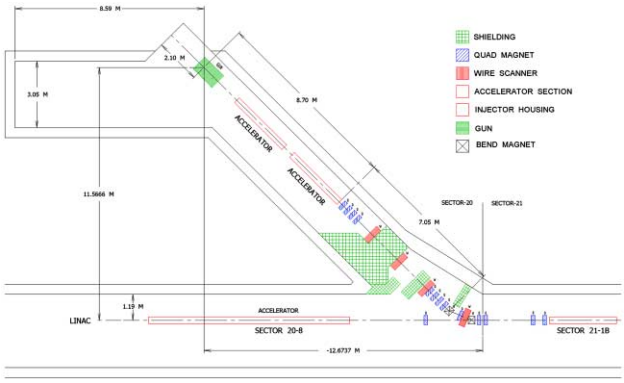

Figure 1. LCLS injector layout with RF-gun at top left. The main (existing) linac starts at 150 MeV after bends at right.

The injector must produce a single, high brightness electron bunch of 1-nC charge, 100-A peak current, and 1-μm normalized emittance, at a repetition rate of 120 Hz. The booster linac (L0) accelerates and emittance compensates the beam to 150 MeV where it is injected into the SLAC linac for acceleration to 14.3 GeV. Calculations with *Parmela* support these goals.

In addition to generating the high brightness electron beam, the injector must serve as a stable base to support the FEL. Specifically, the laser system must reproduce stable, shot-to-shot timing of <1 psec rms (with respect to linac RF phase), and electron bunch charge of <2% rms, over a time scale of a few seconds. Slower variations will be controlled with beam feedback systems.

2.2 Gun Test Facility (GTF)

The injector R&D is being conducted, in part, at the Gun Test Facility (GTF) at SLAC/SSRL [4]. The GTF is housed in the SPEAR synchrotron injector vault and uses a low repetition rate Nd:glass laser to produce photo-electrons from a single-crystal copper cathode. The RF gun is a 1.6-cell S-band gun developed jointly by BNL/SLAC/UCLA [5], and is followed by one 3-meter S-band structure and beam dump with energy analyzing bend.

The LCLS will use a uniform spatial and temporal laser profile, but the GTF presently produces a temporal gaussian, which limits the achievable emittance. The laser intensity restricts the electron charge to <0.5 nC, with a laser pulse of 2-4 ps FWHM, whereas the nominal LCLS pulse length is 10 ps. These limitations will be overcome in the near future. Emittance measurements versus charge at 30 MeV [6] are reproduced in Figure 2 with a cathode field of 110 MV/m and 2-mm diameter laser spot.

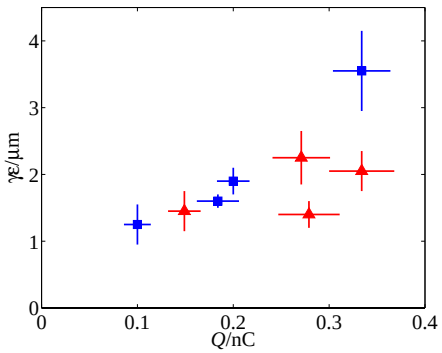

Figure 2. GTF normalized rms emittance vs. charge for 2-ps (square/blue) and 4-ps (triangle/red) FWHM laser pulse. Vertical error bars are an estimate of systematic tail errors.

The measurements show reasonable agreement with *Parmela* calculations. In addition, measurements from BNL/ATF show emittance levels as small as 2.4 μm at 1 nC [7], with more recent results indicating a level of 0.8 μm at 0.5 nC and 60 MeV [8]. But much more work remains to demonstrate a repeatable 1-μm emittance at 1-nC of charge, with routine 120-Hz operation.

3 ACCELERATION & COMPRESSION

3.1 Linac Design

The acceleration and compression systems are incorporated into the last 1-km of the SLAC linac and are designed to produce a 14.3-GeV electron beam with peak current in excess of 3.4 kA. The layout of these systems and some parameters are shown schematically in Figure 3.

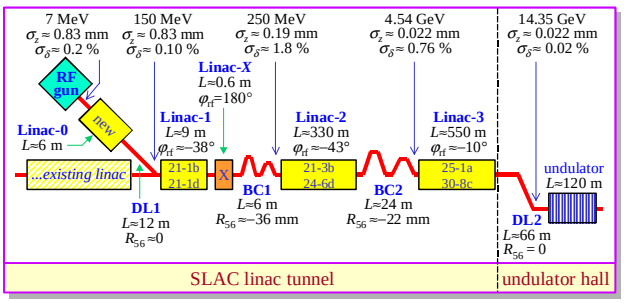

Figure 3. Schematic layout of LCLS acceleration and compression systems (Linac-1 is abbreviated L1,… etc.).

The design includes a two-stage compressor system, S-band RF acceleration, and a short 4th harmonic (X-band) compression RF linearizer section (Linac-*X*) [9]. The results of 2D tracking in longitudinal phase space are shown in Figure 4 at 14.35 GeV at the undulator entrance.

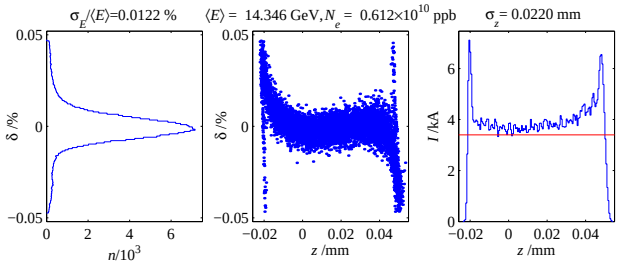

Figure 4. Energy (left) and temporal (right) e^- distributions, and longitudinal phase space (center) at undulator entrance.

3.2 Brightness Preservation

Preservation of beam brightness through these systems is critical. Effects such as transverse wakefields, component misalignments, and coherent synchrotron radiation (CSR) in the various bends can compromise the emittance and increase the SASE saturation length. The design of the acceleration and compression systems has focused on these issues, and includes such features as double-chicane compressors to mitigate the effects of CSR [10]. Bunch length and energy spread values at the various stages, and compressor locations have been optimized to reduce these degrading effects and also to desensitize the system to gun-laser timing and charge variations. Transverse wakefields are reduced in comparison to SLC experience, due to a shorter bunch length, less charge, and fewer RF structures in the LCLS accelerator. These effects, and their possible correction, have been studied in the particle tracking described below and in reference [1].

The effects of CSR in the various bend systems have been modeled using the codes *Elegant* [11] and *TraFiC4* [12]. The temporal profiles used in *Elegant* are based on full system tracking, rather than gaussian beams, with estimated emittance growth levels of <6% in the first compressor (BC1), <25% in the second compressor (BC2), and <6% in the final dog-leg (DL2). In each case the projected emittance is increased, but the time-sliced emittance is nearly unchanged. These calculations are based on the line-charge model of reference [13], which includes field transients before and after each bend. The emittance results are sensitive to possible micro-structure on the bunch and are still very much an R&D issue.

A complete calculation of the CSR emittance growth in a real chicane is not a simple matter. A few experiments have been carried out, with encouraging results (*e.g.*, [14]), but more data and experience is still needed, especially in the LCLS regime. R&D on this critical issue is being carried out, in part, at ANL/APS at the LEUTL facility [15], and possibly at SLAC in the near future [16].

The entire LCLS accelerator, from cathode to undulator entrance, has been modeled using *Parmela* from cathode to main linac entrance at 150 MeV, and using *Elegant* to

the undulator. The 6D tracking is done for 2×10^5 macro-particles and includes: space-charge effects up to 150 MeV; transverse and longitudinal wakefields; CSR effects; incoherent synchrotron radiation in the bends; misaligned quadrupoles, BPMs, and RF structures; and trajectory/emittance correction. Figure 5 shows the slice emittance versus bunch slice number (50 slices) at 150 MeV, and also at the undulator at 14.35 GeV. Slice emittance is preserved to within <10% in the bunch core.

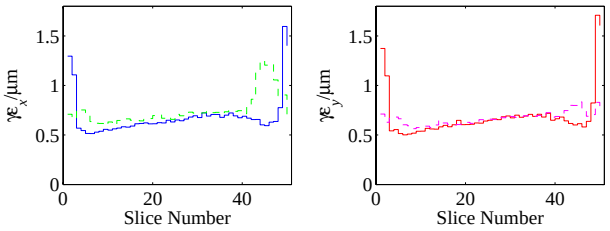

Figure 5. Slice emittances at 150 MeV (solid) and 14.35 GeV (dash) after entire accelerator, including compression, wakes, misalignments, CSR, and correction. Bunch head at slice-1.

The time-sliced beam is input to the FEL code *Genesis-1.3* [17] using the centroid and rms quantities of each slice in 6D, including beta-function variations along the bunch. Resistive and roughness wakefields in the undulator (see next section) are also included. These computer results show saturation well within the undulator length [18], but the simulations are also quite sensitive to the precise CSR and undulator wakefield models.

3.3 Machine Stability

The strong compression imposes tight pulse-to-pulse stability tolerances on RF phase, voltage, gun-laser timing, and bunch charge. A list of 'jitter' tolerances is given in Table 2 where the term "mean" phase (voltage) implies a variation averaged over all klystrons in that linac (L0: 2-klystrons, L1: 1-klystron, L2: 26-klystrons, and L3: 45-klystrons). The required RF stability levels have been verified with measurements [19][20].

Table 2. Pulse-to-pulse rms jitter tolerances for <15% peak current jitter. These are limits on stability at <10-sec time scales.

bunch charge variation	$\Delta Q/Q$	2	%
gun-laser timing	Δt	0.9	psec
L0 & L1 mean RF phase	$\langle\varphi_{0,1}\rangle$	0.1	deg-S
L0 & L1 mean RF voltage	$\langle V_{0,1}\rangle$	0.1	%
L2 & L3 mean RF phase	$\langle\varphi_{2,3}\rangle$	0.07	deg-S
L2 & L3 mean RF voltage	$\langle V_{2,3}\rangle$	0.07	%
L*X* mean RF phase	$\langle\varphi_x\rangle$	0.3	deg-X
L*X* mean RF voltage	$\langle V_x\rangle$	0.25	%

The effects of random, uncorrelated variations of the 12 parameters in the 'jitter budget' have been simulated using repeated 2D particle tracking. Some of the results for 17-seconds of simulated LCLS operation are shown in Figure 6 (tracking 10^5 particles 2000 times with random parameter jitter). Further studies which include all six dimensions of phase space are described in reference [21]. The variation in bunch arrival time is of the order of the bunch length itself (*i.e.*, ~100 fsec rms). This can be mitigated by using pump-probe techniques to measure the relative timing for each FEL pulse [22].

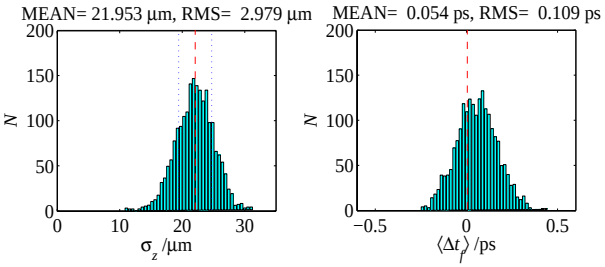

Figure 6. Repeated tracking shows variation of rms bunch length (left) and relative bunch arrival time (right) due to random jitter in linac and injector, according to tolerance budget of Table 2.

Adequate stability of the LCLS will be a very important aspect in understanding, measuring, and correcting machine performance. Feedback systems need to be developed to deal with machine variations on much longer time scales (minutes, hours, and days). These systems will not only control beam energy and transverse oscillations, as at the SLC [23], but will also need to maintain the final bunch length. To this end, a transverse S-band RF deflecting structure will be used after BC2 (and possibly after BC1) to steal pulses at ~1 Hz and 'streak' the beam onto a profile monitor [24]. The beam size measurement is easily related to the absolute bunch length, and a 22-μm length is well measured with a 20 MV RF field. A feedback system will be developed to maintain both energy and bunch length after the chicanes. Such a system has not been developed or tested yet, but an existing 2.4-m RF deflecting structure from the 1960's has been installed in the SLAC linac for initial testing. The 'slice' emittance and 'slice' energy spread can also be measured with the streaked beam from the deflector.

4 UNDULATOR

4.1 LCLS Undulator Design

The LCLS undulator is a planar, permanent-magnet hybrid array, with 30-mm period and 6-mm fixed gap [25]. The design uses proven hybrid technology of vanadium-permendur poles and Nd-Fe-B magnets. Helical and superconducting options are presently seen as too costly and complex, with untested aspects such as mechanical tolerances, steering correction, and limited beam-pipe access. Some parameters are given in Table 3.

A FODO focusing array is incorporated by adding section breaks, of two lengths, between modular 3.4-m undulator sections. Electron beam diagnostics will be added at the breaks, with every third break longer to

include photon beam diagnostics. Quadrupole focusing elements are permanent magnets with inverse focal length 0.112 m^{-1} ($\langle\beta\rangle \approx 18$ m). Each quadrupole will be mounted on remotely controlled magnet movers with independent horizontal and vertical position control. The undulator sections will also be mounted on moveable stages with five degrees of freedom (x and y position, pitch, yaw, and roll). Piezo translator stages are included at magnet array terminations to allow phasing adjustment at the breaks.

Table 3. LCLS undulator parameters.

undulator line physical length	L_u	122	m
undulator period	λ_u	30	mm
undulator parameter	K	3.71	
undulator section length	L_s	3.42	m
magnetic gap height	g	6.0	mm
number of undulator sections	N_s	33	
break length (short)	ΔL_1	0.187	m
break length (long)	ΔL_2	0.421	m

A beam position monitor (BPM) of ≤1-μm resolution will be located adjacent to each quadrupole. The BPM will be a combination of button-style pickup electrodes with a cavity-based pickup all in one compact assembly. This preserves the high resolution capability of the cavity system and eliminates the need for a reference phase signal to determine the sign of the position measurement. A schematic of the LCLS undulator is shown in Figure 7.

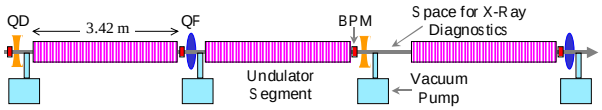

Figure 7. One of 11 LCLS undulator line super-periods.

A prototype 3.4-m undulator section has been fabricated at ANL/APS [26]. A 9-pole section is shown in Figure 8.

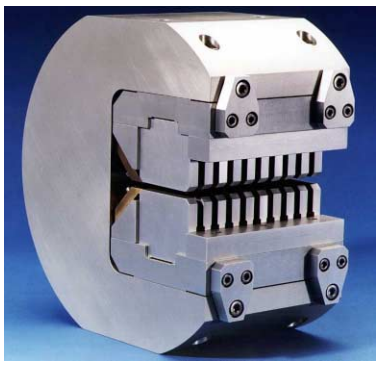

Figure 8. Short (9 pole) undulator section prototype with titanium C-shape support structure and thermal compensation.

The design emphasizes mechanical stability against thermal and support variations using a 12-inch diameter titanium C-shape support structure. The low thermal expansion of titanium limits the length variation to a tolerable 30 μm/deg-C, but the remanent field of Nd-Fe-B magnets decreases by ~0.1% per deg-C temperature rise. This is compensated by providing a machined aluminum base-plate between the titanium core and the magnet/pole assemblies to reduce the gap in proportion to the field reduction with increased temperature. The pole gap tolerance is 3 μm, which will be controlled during fabrication using field measurements and shimming techniques. The demanding trajectory alignment of <5 μm will be accomplished using beam-based techniques [27].

4.2 Wakefields in the Undulator

The 6-mm undulator gap necessitates a long, cylindrical vacuum pipe with inside radius of just 2.5 mm. The electron beam interaction with the narrow undulator vacuum chamber can generate an energy gradient across the bunch, concurrent with the SASE process, which can potentially reduce the FEL gain. These wakefields are influenced by both beam pipe surface roughness and conductivity, and increase in amplitude with a shorter bunch length and higher charge. The limits for the wakefield energy spread, generated *within* the LCLS undulator, are <0.1% rms. The resistive-wall wake [28] can be reduced to a level below this by plating the beam pipe with copper. Wall roughness limits, however, require consideration of the surface character. Surface profile measurements of an undulator pipe using an atomic force microscope [29] have revealed a long wavelength character of typical surfaces with roughness amplitude (radial) much smaller than its length (longitudinal). Recent analysis, which includes the high 'aspect-ratio' character of the roughness [30], indicates that the energy spread can be held to <0.001% with a surface finish of 0.2 μm rms if the roughness length is ≥100 μm, which is typical. Plans are in place to make direct measurements of this effect at the SLAC/SSRL Gun Test Facility.

5 *X*-RAY OPTICS

The LCLS *x*-ray optics R&D program encompasses a number of fundamental and technical areas. The former include theoretical and numerical investigations of radiation-matter interactions in the strong field regime, the phase space structure of LCLS radiation pulses, and diffraction and coherence propagation in the ultra short pulse regime. Practical areas include the development of *x*-ray optics for tailoring of the phase space of LCLS pulses (e.g., microfocusers, attenuators, temporal compressors, slicers, etc.) and for their characterization (e.g., spectrometers, calorimeters, interferometers, etc.). The R&D program is being pursued at LLNL and SLAC.

6 RELATED WORK

6.1 Toward Shorter X-ray Pulses

There is a good deal of interest in further shortening the LCLS *x*-ray pulse to well below the nominal full-width

value of 230 fsec. The primary motivation is to allow *x*-ray image capture before molecular damage occurs in the sample from intense radiation. One of the most promising ways to achieve a significantly shorter pulse is with a chirped-beam, two-stage undulator scheme [31], [32]. The electron beam is shaped with a linear energy-time correlation so that the *x*-ray pulse generated in the first undulator stage is similarly chirped. A monochromator placed in an electron bypass (a magnetic chicane) selects a narrow bandwidth which, due to the correlation, greatly narrows the pulse width. This shortened *x*-ray pulse is then used to seed a second stage undulator to SASE saturation. The result is an *x*-ray pulse of <10 fsec full-width, while the monochromator also effectively masks shot-to-shot e^- energy fluctuations.

6.2 SASE at TTF-FEL, LEUTL and VISA

A large portion of the initial LCLS R&D plans was reserved for the experimental demonstration of SASE saturation. To this end, a visible to infrared SASE amplifier FEL experiment (VISA), supported by the BNL Accelerator Test Facility (ATF), was built with a 4-m undulator and discrete focusing. During VISA commissioning, the TTF-FEL at DESY observed SASE gain in February of 2000 at a 109-nm wavelength, and the Low Energy Undulator Test Line (LEUTL) at ANL/APS successfully demonstrated SASE saturation at 530 and 390 nm in September 2000 [33].

VISA successfully reached SASE saturation at 840 nm in March 2001 [34] with a gain of 2×10^7, and a gain length of 18.7 cm. These various experiments will continue to provide increased understanding and indispensable hands-on experience with SASE FELs.

6.3 Future Short Pulse Generation at SLAC

At SLAC, a proposal is being assembled for a facility to produce extremely short electron bunches of 30-kA peak currents [16], for accelerator research and to initiate an ultra-short *x*-ray science program at SLAC based on spontaneous radiation in a 10-m undulator. With a new magnetic chicane in the linac, electrons from the existing damping ring will be compressed in three stages, with the final stage provided by the existing Final Focus Test Beam (FFTB). With a bunch length <100 fsec, this facility can provide needed R&D for the LCLS accelerator and *x*-ray optics, and greatly strengthen the LCLS design.

7 ACKNOWLEDGEMENTS

This publication represents the work of a large group of people at the collaborating institutions working towards a future *x*-ray FEL.

8 REFERENCES

[1] LCLS Design Study Report, SLAC-R-521, (1998).
[2] H.-D. Nuhn, "Technological Challenges to X-Ray FELs", *22nd International Free Electron Laser Conf.*, Aug. 2000, Durham, NC, USA.
[3] D.T. Palmer, "The Next Generation Photoinjector", Ph.D. dissertation, Stanford University, 1998.
[4] J. Schmerge, et. al., *SPIE* 3614 (1999) 22.
[5] D.T. Palmer, et. al., *1997 Part. Accel. Conf.*, Vancouver, BC, Canada, p. 2687.
[6] P.A. Bolton, et. al., LCLS-TN-01-04R, June 2001.
[7] M. Babzien, et. al., "Observation of Self-Amplified Spontaneous Emission in the Near Infrared and Visible", *Phys. Rev. E* 57 (1998) 6093.
[8] V. Yakimenko et. al., to be published at FEL2001.
[9] P. Emma, LCLS-TN-01-01, to be published.
[10] P. Emma, R. Brinkmann, *1997 Part. Accel. Conf.*, Vancouver, BC, Canada, p. 1679.
[11] M. Borland, *ICAP-2000*, Darmstadt, Germany, Sep. 2000.
[12] M. Dohlus, T. Limberg, *XVIII International Free Electron Laser Conference* (Rome, 1996).
[13] E. L. Saldin, E. A. Schneidmiller, M. V. Yurkov, "On the Coherent Radiation of an Electron Bunch Moving in an Arc of a Circle", TESLA-FEL 96-14, Nov. 1996.
[14] H.H. Braun, et. al., *Proc. of the 20th International Linac Conf.*, Monterey, California, 21-25 Aug 2000.
[15] M. Borland, et. al., "Initial Characterization of Coherent Synchrotron Radiation Effects in the Advanced Photon Source Bunch Compressor", these proceedings.
[16] P. Emma, et. al., "Femtosecond Electron Bunch Lengths in the SLAC FFTB Beamline", these proceedings.
[17] S. Reiche et. al., Nucl. Inst. & Meth. A429 (1999) 243.
[18] S. Reiche et. al., these proceedings.
[19] R. Akre et. al., *Proc. of the 20th International Linac Conf.*, Monterey, California, 21-25 Aug 2000.
[20] R. Akre et. al., these proceedings.
[21] M. Borland, et. al., "Start-to-End Jitter Simulations of the Linac Coherent Light Source", these proceedings.
[22] B. Faatz, et. al., DESY-TESLA-FEL-2000-05D.
[23] T. Himel, et. al., *1993 Part. Accel. Conf.*, Washington, DC., May 1993, p. 2106.
[24] P. Krejcik, et. al., "A Transverse RF Deflecting Structure for Bunch Length and Phase Space Diagnostics", these proceedings.
[25] E. Gluskin, et. al., "Optimization of the Design of the LCLS Undulator Line", *22nd International Free Electron Laser Conf.*, Aug. 2000, Durham, NC, USA.
[26] E. Moog, et. al., "Design and Manufacture of a Prototype Undulator for the LCLS Project", these proceedings.
[27] P. Emma, et. al., "Beam Based Alignment for the LCLS FEL Undulator", *20th International Free Electron Laser Conf.* (FEL 98), Williamsburg, VA, 16-21 Aug 1998.
[28] K.L.F. Bane, M. Sands, "The Short-Range Resistive Wall Wakefields", SLAC-PUB-7074, Dec. 1995.
[29] G. Stupakov, et. al., "Effects of Beam Tube Roughness on X-ray FEL Performance", *Phys. Rev. ST Accel. Beams* 2, 060701 (1999).
[30] G. Stupakov, "Surface Roughness Impedance", *Physics of, and Science with, the X-ray Free Electron Laser*, Sep. 2000, Arcidosso, Italy.
[31] J. Feldhaus, et. al., Opt. Comm. 140 (1997) 341.
[32] C. Schroeder, et. al., "Two-Stage Chirped-Beam SASE-FEL for High Power Femtosecond X-ray Pulse", these proceedings.
[33] S.V. Milton et al., "Exponential Gain and Saturation of a Self-Amplified Spontaneous Emission FEL", Science 10.1126/science.1059955, Published Online May 17, 2001.
[34] A. Tremaine, et. al., "Measurements of an 800-nm SASE FEL", these proceedings.